Soft Matter

PAPER

View Article Online
View Journal | View Issue

Cite this: *Soft Matter*, 2019, **15**, 3929

Aggregation dynamics of active rotating particles in dense passive media

Juan L. Aragones, †[a] Joshua P. Steimel†[b] and Alfredo Alexander-Katz*[c]

Active matter systems are able to exhibit emergent non-equilibrium behavior due to activity-induced effective interactions between the active particles. Here we study the aggregation and dynamical behavior of active rotating particles, spinners, embedded in 2D passive colloidal monolayers. Using both experiments and simulations we observe aggregation of active particles or spinners whose behavior resembles classical 2D Cahn–Hilliard coarsening. The aggregation behavior and spinner attraction depend on the mechanical properties of the passive monolayer and the activity of spinners. Spinner aggregation only occurs when the passive monolayer behaves elastically and when the spinner activity exceeds a minimum activity threshold. Interestingly, for the spinner concentrations investigated here, the spinner concentration does not seem to change the dynamics of the aggregation behavior. There is a characteristic cluster size which maximizes spinner aggregation by minimizing the drag through the passive monolayer and maximizing the stress applied on the passive medium. We also show a ternary mixture of passive particles and co-rotating and counter-rotating spinners that aggregate into clusters of co and counter-rotating spinners respectively.

Received 29th October 2018,
Accepted 9th April 2019

DOI: 10.1039/c8sm02207k

rsc.li/soft-matter-journal

1 Introduction

Attractive interactions between particles in a homogeneous mixture induce the formation of clusters. These clusters grow in time until the mixture separates into two distinct phases. The dynamics of phase separation in binary mixtures is well characterized[1–3] and depends on the dimensionality, thermodynamic conditions, and type of cluster growth, diffusion or source/interface limited. Often, these attractive interactions are induced by direct chemical interactions. Alternatively, they can also be induced by electromagnetic, phoretic,[4] collision[5] or hydrodynamic forces.[6–8] Non-equilibrium interactions can also promote particle aggregation. Due to the non-equilibrium nature of active matter systems, these are excellent candidates to study novel mechanisms of particle aggregation and subsequent phase separation that may deviate from traditional Cahn–Hilliard models.

Active matter systems are composed of active agents that consume energy from their environment and convert it into motion or mechanical forces. The most prominent examples of these active systems are living organisms, which exhibit striking emergent non-equilibrium behaviors such as swarming, lining, vortexes, *etc.*[9–23] Synthetic active systems that are able to mimic and reproduce some of the emergent behavior exhibited by living organisms can be used as model systems to study the underlying physical principles which govern their behavior. These synthetic active systems are composed of active units that locally convert energy into motion. This activity perpetually drives these systems out-of-equilibrium. Alternatively, activity can also be induced *via* an externally applied field or stimuli, some examples of which include magnetic or electric fields, light-catalyzed chemical reactions, vibrating granular beds and optical tweezers.[24–26] One particular mode of activity, rotation in plane, has recently aroused a great deal of interest for synthetic and simulation active matter studies. These systems of micro-rotors or spinning particles have been studied in theory and simulations[27–31] using magnetic particles,[24,32] Janus particles,[25,33] rotating robots[34] and even some biological systems[35] as the active units. Almost all of these studies report some type of emergent non-equilibrium steady state where aggregation or phase separation occurs and most of the analysis tends to focus on the dynamics of the active units, the structure or order of the aggregate or active matter system, the origin of the aggregation (typically *via* some type of cooperative alignment of the active units) and developing a phase diagram of the emergent non-equilibrium steady states as a function of the activity or density of the active units. There have been very few studies that investigate and characterize the dynamics of these active rotating aggregates in

[a] *Departamento de Física Teórica de la Materia Condensada, Instituto Nicolás Cabrera and Condensed Matter Physics Center (IFIMAC), Universidad Autónoma de Madrid, E-28049 Madrid, Spain. E-mail: juan.aragones@uam.es*
[b] *School of Engineering and Computer Science, University of the Pacific, Stockton, CA, 95219, USA. E-mail: jsteimel@pacific.edu*
[c] *Department of Materials Science and Engineering, Massachusetts Institute of Technology, Cambridge, MA, 02139, USA. E-mail: aalexand@mit.edu*
† These authors contributed equally to this work.

terms of the evolution of the cluster size as a function of time and as a function of activity, active particle concentration, and area fraction of the monolayer in order to compare the phase separation behavior of active systems to traditional Cahn–Hilliard behavior. Additionally, in most research works these spinning active systems contain only active components. This is problematic as most biological systems or processes are not composed of purely active components. In biological systems the active or motile components, *i.e.* cells, are often surrounded by immobile, passive, or even abiotic interfaces. Investigating emergent non-equilbrium behavior and characterizing the aggregation dynamics in such an artificial model system composed of active and passive components can potentially help distinguish which biological interactions can be attributed to purely physical phenomena and which interactions require presumably physical and biological/biochemical stimuli.

Here, we study a model active matter system that is composed of both passive and active components to study the aggregation of active particles. The active component in this system is superparamagnetic particles embedded in a dense monolayer of passive particles. The superparamagnetic particles are made active upon actuation of an externally rotating magnetic field (around the axis perpendicular to the monolayer) causing the particles to spin, henceforth referred to as spinners and schematically shown in Fig. 1A. In this system, active particles exhibit a long-range attractive interaction,[36,37] which emerges from the non-equilibrium nature of the system and is mediated by the mechanical properties of the passive medium. We observe that spinners embedded in a dense passive monolayer tend to aggregate forming clusters which grow in time, as schematically shown in Fig. 1. By means of experiments and numerical simulations we demonstrate that this spinner aggregation is driven by the non-equilibrium attractive interaction induced by the mechanical properties of the passive matrix. Moreover, we show that the spinner aggregation process follows a dynamics that resembles spinodal decomposition in passive liquids and coalescence. The dynamics of the aggregation process depends on the mechanical properties of the monolayer as well as the activity of the spinners. This type of non-equilibrium attractive interaction opens the door to controlling the state of the system *via* control of the mechanical properties of the medium, the activity of the spinners, and the density of the spinners.

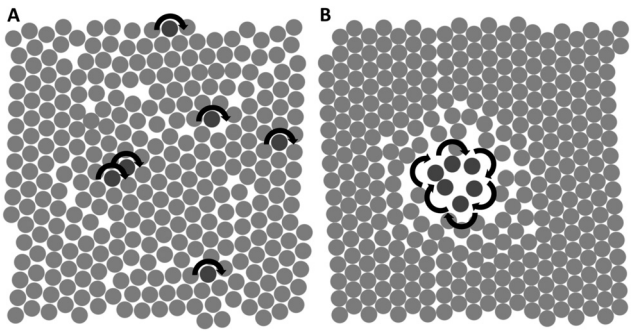

Fig. 1 Schematic representation of the system. (A) Co-rotating spinners randomly distributed within a monolayer of passive particles of $\phi_A = 0.8$, which under the action of the magnetic field rotate around the axis perpendicular to the monolayer plane (*i.e.* the z-axis). (B) Spinner clusters form due to attraction between active particles.

2 Materials and methods

2.1 Experiments

Our synthetic model system is composed of active spinning particles and passive particles. The spinners are superparamagnetic polymer-based magnetite particles purchased from Bangs Laboratories, while the passive particles are composed of polystyrene purchased from Phosphorex; both, active and passive, are 3 μm in diameter. We use a concentrated solution of spinners, $\approx 4\ \mu g\ mL^{-1}$, and passive particles, $\approx 0.8\ mg\ mL^{-1}$, to study the aggregation and dynamical behavior of the spinners. The spinners are made active by externally applying a magnetic field which rotates around the axis perpendicular to the plane of the monolayer. The solution of spinners and passive particles is inserted into a channel (22 mm (L) × 3 mm (W) × 300 μm (H)), fabricated using a glass slide, spacer, and cover slip. Once the solution is inserted into the channel it is sealed with epoxy and allowed to sediment for 10 minutes to form a dense monolayer, before being magnetically actuated. Using particles rolling on a glass slide we demonstrate that there is no interaction between the spinner and the wall. These particles rolling on a glass substrate translate at much lower velocities, close to the limit where the only friction that occurs is due to hydrodynamics. The strength of the magnetic field is 5 mT, which is large enough to maintain alignment of the superparamagnetic particles with the rotational frequency of the field. The magnetic field is actuated at an angular frequency, ω, of 5 Hz for approximately 10 minutes, with the rotational sense switched every 2 minutes. This rotational frequency corresponds to $Re = 1.25 \times 10^{-6}$. The combination of the strength of the applied field and the rotational frequency used imparted enough activity to the superparamagnetic particles to induce the emergent attractive interaction mediated by the elastic passive medium. Ferromagnetic particles can also be used as the active unit alternatively and similar aggregation behavior is observed.

2.2 Simulations

In addition, we carry out numerical simulations of this system. In particular our coarse grained model consists of pseudo-hard sphere particles,[38] $N = 324$, suspended in a fluid of density $\rho = 1$ and kinetic viscosity $\nu = 1/6$ modeled using the lattice-Boltzmann method. We use the fluctuating lattice-Boltzmann equation[39] with $k_BT = 2 \times 10^{-5}$ and the solver D3Q19. We discretized the simulation box in a three dimensional grid of $N_x \times N_y \times N_z = 101 \times 101 \times 20$ bounded in the z direction by no-slip walls and periodic boundary conditions in the x and y directions. We set the grid spacing, Δx, and time step, Δt, equal to unity. The particles are treated as real solid objects[40] of diameter $\sigma = 4\Delta x$. The momentum exchange between the fluid and solid particles is calculated following a moving boundary condition,[41] which allows us to calculate the forces and torques

exerted on the particles from the momentum transferred from the fluid. The particles settle on the bottom wall of the channel forming a monolayer under the action of a gravitational force, F_G = 0.005. The activity is achieved by imposing a constant torque, which in general corresponds to Re = 0.72, unless otherwise noted.

3 Results and discussion

To investigate the emergent aggregation behavior of active rotating particles embedded in monolayers of passive particles, we created a dense passive monolayer of inactive polystyrene particles with a particle area fraction, ϕ_A, of approximately $\phi_A \approx 0.7$. The passive monolayer was doped with active superparamagnetic particles so that the particle fraction of the active component was approximately 0.5%. Upon actuation of the magnetic field, we observe that spinners aggregate forming nearly circular actively rotating clusters, whose average radius, $\langle R_{cluster} \rangle$, grows with time, as shown in Fig. 2A. These clusters of spinners can be seen growing over time in the experimental snapshots at the top of Fig. 2A, where the spinners are the darker regions in the snapshots. This behavior is markedly different from that observed in a system of purely active superparamagnetic and ferromagnetic particles,[42–47] as shown in Fig. 2B. At similar particle area fractions and rotational frequencies in the purely active system the aggregation of particles is dominated by magnetic dipole–dipole interactions.[36,37] This magnetic force decays as r^{-4} so aggregation will only occur between clusters that are initially very close together. We observe the formation of small chains or random aggregates that slightly grow with time due to fluid flow induced motion, as seen in Fig. 2B. However, there is no emergent long range attractive interaction that drives spinner aggregation in the purely active case and as a result the spinner aggregation is much slower; a phenomenon observed in other similar systems.[46,47] This emergent increase in aggregation growth is counter-intuitive because in pure equilibrium arguments one would expect the monolayer to impede aggregation because of the high viscosity of the media.

We conducted numerical simulations of this system to study the role of the passive matrix in the spinner aggregation process, and consider whether magnetic dipole–dipole interactions play a major role in the spinner aggregation process, particularly at large cluster sizes. Therefore, our coarse grained model neglects the dipole–dipole interactions to isolate the effect of the passive matrix in the spinner aggregation process. In agreement with the experimental results we observe that spinners aggregate forming circular clusters when embedded in dense monolayers of passive particles of ϕ_A = 0.8. We calculate the time evolution of the area of the active clusters, $A(t)$, for the experimental and simulation trajectories, as shown in Fig. 3. We again observe that the size of the clusters grows with time. Hence, the presence of the passive monolayer promotes aggregation of the spinners, even in the absence of magnetic dipole–dipole interactions. Interestingly, we find that $A(t) \propto t^{1/2}$ for the simulations and $A(t) \propto t^{0.37}$ for the experimental system. For a classical Cahn–Hilliard spinodal

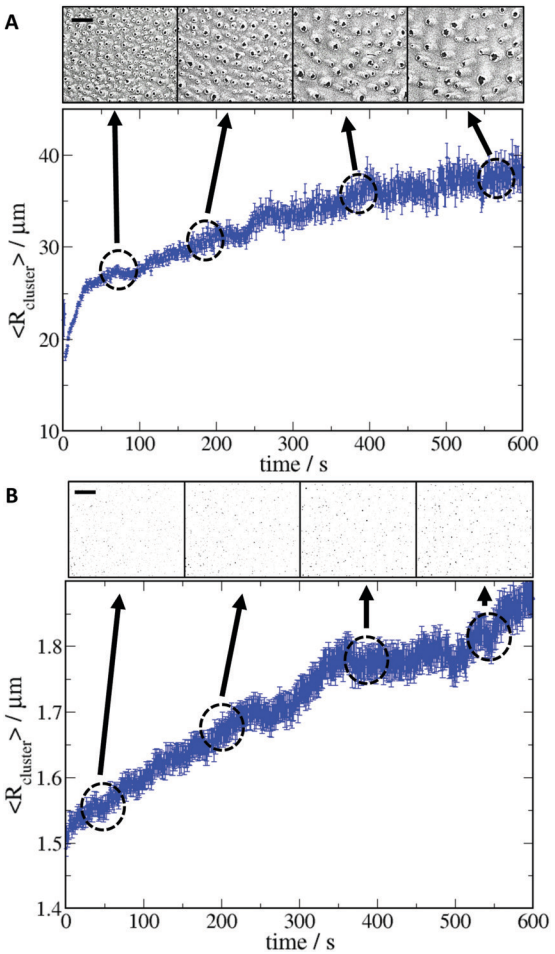

Fig. 2 Average spinner cluster radius, $\langle R_{cluster} \rangle$, as a function of time for the hybrid active–passive (A) and the purely active system (B). The experimental snapshots show the aggregation of spinners as a function of time for each system. The spinners correspond to the darker spots. The scale bar in the left snapshot corresponds to 100 μm.

decomposition scenario in 2D, one would expect that the characteristic length of the clusters of active particles will scale as $t^{1/3}$ in the case of diffusion-limited coarsening or as $t^{1/2}$ in the case of interface/source-limited coarsening. In diffusion-limited coarsening, the cluster–matrix interface acts as a sink and maintains the concentration of particles at the interface and thus the aggregation is determined by the rate of diffusion of particles towards the clusters. On the contrary, in the interface-limited case the diffusion of particles is fast and the limiting factor is the interface, which acts as a poor sink, not accommodating incoming particles quickly enough. Our simulation results appear to place us in the interface or source-limited scenario while our experimental scaling law is closer to the diffusion limited case, which may be due to the lack of magnetic dipole–dipole interactions in the simulation. The absence of dipole–dipole interactions induces fluctuations in the time evolution of the domain length, $A(t)$. When two clusters collide, the clusters split into pieces and while the new merged cluster is re-configuring the size of the clusters fluctuates.

There have been a number of purely active simulation systems that have found the interface limited scenario scaling

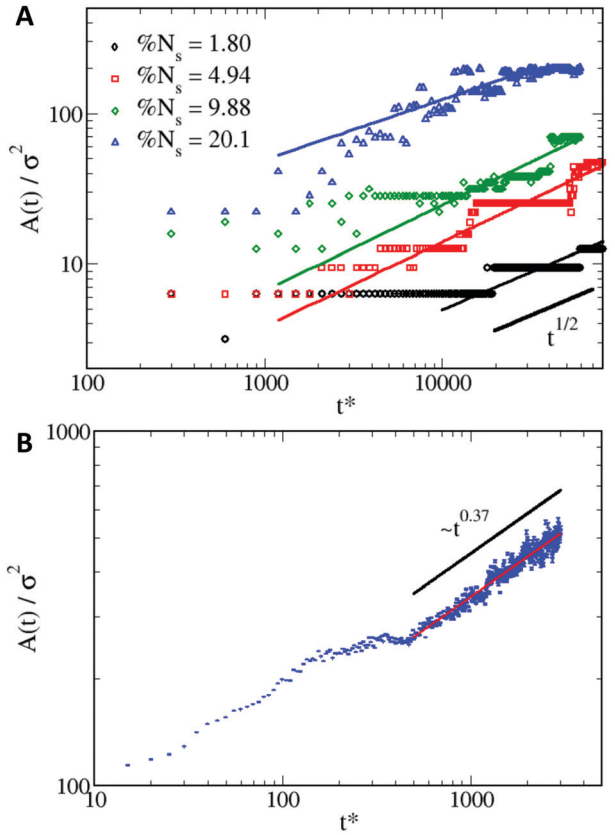

Fig. 3 (A) log–log scale for the spinner cluster size (area), $A(t)$, as a function of time in a passive monolayer of ϕ_A = 0.8 for four different spinner concentrations: 1.8% (black circles), 4.94% (red squares), 9.88% (green diamonds) and 20.1% (blue triangles) in simulations. (B) log–log scale for the spinner cluster length from experiments as a function of time in a passive monolayer of $\phi_A \approx 0.7$. t^* corresponds to the dimensionless time $t \cdot \omega$ and the cluster area is scaled by the square particle diameter, σ^2.

of $t^{1/2}$, although the origin of this scaling behavior is still unclear.[48,49] Recently, a micro-rotor system with spinning robots as the active unit exhibited a characteristic length which scaled as $t^{1/3}$, the diffusion limited scenario.[34] However, as a difference from previous studies that only considered purely active systems, our system is composed of both active and passive components. What seems clear is that the aggregation dynamics of spinners is enhanced by the presence of the dense passive monolayer when compared to the purely active spinner system. The scaling behavior in the purely active system is about 0.012, in agreement with previous results.[46,47] The difference is even more pronounced with another system at similar field strengths but higher rotational frequencies where the scaling factor of $t^{0.37}$ is orders of magnitudes larger.[46,47]

This stark difference in aggregation dynamics between the purely active and hybrid system is due to a recent result where we showed that an attractive interaction emerges between two co-rotating particles, or spinners, if embedded in dense passive monolayers.[36,37] This emergent attractive interaction and the subsequent non-equilibrium phase separation are thus mediated by the elasticity of the medium and the ability of the spinners to stress that medium. Under the actuation of the rotating magnetic field, the spinners rotate around the axis perpendicular to the substrate generating a rotational fluid flow.[50–52] This causes the surrounding passive particles to rotate due to the momentum transferred through the fluid in which the particles are suspended. In addition, at small but finite Re, the spinner's rotational motion produces a so-called secondary flow due to the fluid inertia, which pushes away the nearest shell of passive particles, effectively compressing the passive monolayer. Thus, two co-rotating spinners apply compressive and shear stresses on the passive particles located in between the spinners, referred to as the bridge. This produces a stochastic, but steady degradation of the bridge, which allows the spinners to approach, resulting in an attractive interaction.[36] Moreover, depending on the mechanical properties of the passive monolayer, this attractive interaction between active rotating particles may be of a very long-range nature.[37]

The solid-like character of the passive monolayer induces an attractive interaction between the active particles resulting in the aggregation of the spinners embedded in passive matrixes. However, we do not observe the complete phase separation of the system into passive and active domains for the actuation time period investigated. Instead, spinners aggregate forming clusters which grow with time embedded within the passive matrix. The dynamics of this aggregation process resembles spinodal decomposition, in which active clusters coalesce. From the experimental trajectories we compute the time evolution of the number of active clusters, $N(t)$, as shown in Fig. 4A. We observe two different dynamical regimes within the experimental time scale. At short time scales (less than 100 s) the clusters exhibit an initial regime of slow cluster growth, or an almost constant number of clusters. This makes sense as we previously determined that the characteristic time scale of continuous activity, at a rotational frequency of 5 Hz, to induce the emergent long range attractive interaction between spinners is on the order of 10–100 s. So this slow growth regime appears because the spinners must first stress the elastic medium before the attractive interaction that drives aggregation emerges. This is followed by another regime (after 100 s) where the spinners aggregate at a much faster rate. As it can be seen in Fig. 4A, the scaling of the number of clusters with time in this regime is characterized by an exponent of ≈ -0.7. We also analyze the dynamic scaling of the aggregation of spinners in our simulation model. In this case, we also observe two dynamical regimes: an initial slow decrease in the number of clusters (*i.e.* growth of the cluster sizes), followed by a regime with dynamic scaling of exponent ≈ -0.5, as shown in Fig. 4B. Moreover, this dynamic scaling seems independent of the spinner concentration. The $t^{1/2}$ dynamical scaling of the cluster growth has been observed in simulations conducted by Vicsek and several distinct purely active systems, although the origin of this scaling behavior is still unclear.[48,49] However, we believe that the origin of this scaling behavior is similar to that observed in traditional 2D coarsening[53,54] in the source or interface limited case. Interestingly the slow growth regime scaling seems to correspond to the diffusion limited coarsening case but we actually see enhanced scaling beyond the source

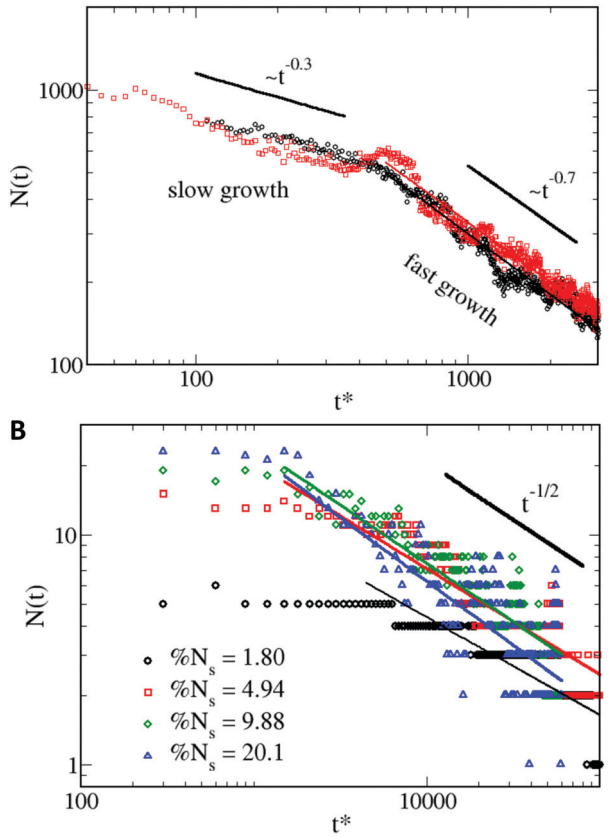

Fig. 4 (A) log–log scale for the number of clusters as a function of time as obtained from the experiments at $\phi_A \approx 0.7$. The two sets of data correspond to two independent experiments. (B) log–log scale for the number of clusters as a function of time as obtained from the simulation model for four different spinner concentrations at ϕ_A = 0.8: 1.8% (black circles), 4.94% (red squares), 9.88% (green diamonds) and 20.1% (blue triangles). t^* corresponds to the dimensionless time $t{\cdot}\omega$.

limited scenario which must be due to the emergent interaction induced by the presence of the dense passive monolayer.

We hypothesize that the difference between the exponents of the dynamic scaling observed in experiments and simulations is due to the magnetic interaction between clusters of spinners, which increases the strength of the spinner–spinner attraction at short distances. Additionally, this also helps to stabilize spinner clusters. If we also assume a dynamic scaling factor for the slower initial regime in the spinner aggregation process, we obtain for experiments and simulations exponents $\approx$0.29(2) and $\approx$0.04(5), respectively. In this first aggregation regime the differences between the experimental and simulation dynamic scaling exponents are much greater than for the second regime. This behavior is in agreement with our hypothesis that the effect of the magnetic dipole–dipole interactions significantly increases the spinner aggregation dynamics. At the beginning of the aggregation process, active particles that are close to one another (less than 4 particle diameters apart) will form a cluster almost instantaneously upon application of the external magnetic field. Also, when active clusters are small the dipoles of the particles are more easily aligned, which results in higher magnetization of the clusters. In contrast, as the size of the clusters increases, some of the dipoles of the particles are frustrated by the cluster structure, which results in a smaller magnetization of the clusters as their size increases. Therefore, the magnetic interaction is more relevant between smaller clusters than between bigger clusters.

The mechanical properties of the passive media determine the interaction between the spinners and thus the dynamics of the spinner aggregation. The mechanical properties of the monolayer can be calculated by measuring the mean square displacement (MSD) of the particles in the monolayer in the absence of active particles, specifically the storage and loss moduli, G' and G'', respectively.[55,56] In simulations, we observe that monolayers of hard-sphere particles at area fractions $\phi_A > 0.7$ respond as viscoelastic materials, behaving as a viscous system at low frequencies and as a solid-like material at high frequencies.[36] However, for $\phi_A < 0.7$ the monolayer behaves as a viscous material over the entire frequency range. To study the effect of the mechanical properties of the monolayer on the dynamics of the spinner aggregation, we investigate, by means of our simulation model, spinners embedded in passive monolayers at different particle area fractions ϕ_A = 0.5, 0.7, and 0.8. As can be seen in Fig. 5, spinners in monolayers of a particle area fraction of ϕ_A = 0.8 and 0.7 follow similar scaling laws. However, at an area fraction of ϕ_A = 0.5, the spinners do not aggregate within the simulation time scale, as shown by the green diamonds in Fig. 5. The small amount of spinner aggregation observed in Fig. 5 is due to spinners being initially positioned together or close enough so that the removal of a single passive row of particles was required. It should also be noted that for a more dilute concentration of spinners no aggregation is observed on the simulation timescale (data not shown). In addition, at these particle area fractions the monolayer is unable to maintain spinners within a cluster and thus the number of clusters exhibits large fluctuations. Thus, the presence of a passive monolayer that behaves as a solid-like material induces an attractive interaction between the active rotating particles, which results in aggregation of spinners. Interestingly, the dynamics of the spinner aggregation seems to be independent of the storage modulus, G', which is higher for a monolayer of ϕ_A = 0.8 than for a monolayer of ϕ_A = 0.7. This might be due to canceling of two competing effects. On one hand, the effective interaction grows with G', but on the other hand the motion of the medium is controlled by η, which also grows.

For spinners in a passive monolayer with a packing fraction $\phi_A > 0.7$ the mechanics of the passive monolayer also plays an important role in keeping the cluster of active particles together. We have previously reported that for a system composed of purely active particles the spinners will repel due to the secondary flows generated by the spinners.[36,57] The spinners within the cluster should then repel, but the passive monolayer exerts a force on the spinners that serves to stabilize the active cluster. This is evident from the stochastic fluctuations shown in the cluster size time evolution, as shown in Fig. 3B and 5, which correspond to clusters breaking and reforming during the aggregation process. The size of the fluctuations increases with the spinners' concentration, due to the bigger size of the clusters.

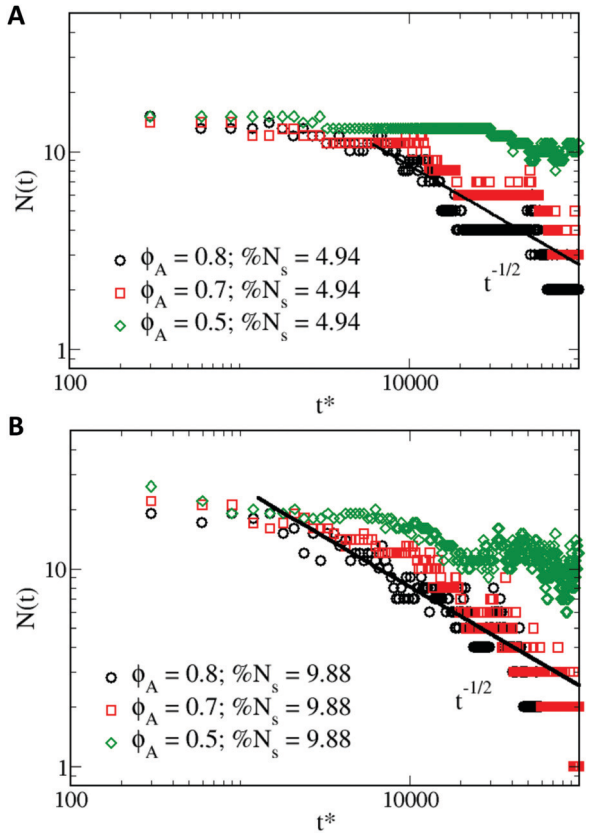

Fig. 5 (A) log–log scale of the time evolution of the number of active clusters at Re = 0.72 and a spinner concentration of 4.94% within passive monolayers of ϕ_A = 0.8 (blue squares), 0.7 (red circles) and 0.5 (green diamonds). (B) log–log scale of the time evolution of the number of active clusters at Re = 0.72 and a spinner concentration of 9.88% within passive monolayers of ϕ_A = 0.8 (blue squares), 0.7 (red circles) and 0.5 (green diamonds). t^* corresponds to the dimensionless time $t{\cdot}\omega$.

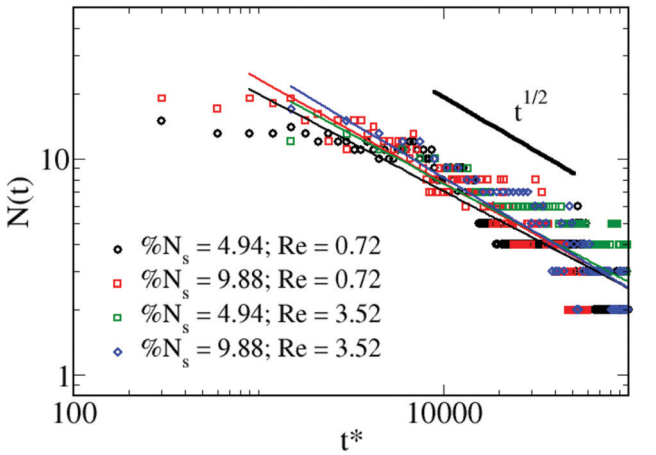

Fig. 6 Aggregation dynamics of spinners within passive monolayers of ϕ_A = 0.8 at two different rotational frequencies Re = 0.72 (black and red symbols) and 3.58 (blue and green symbols) and spinner concentrations 4.94% (circles and diamonds) and 9.88% (squares and triangles). t^* corresponds to the dimensionless time $t{\cdot}\omega$.

Aside from the mechanical properties of the monolayer, the other requisite for spinner attraction is the ability to stress the passive monolayer. Therefore, we also explore the effect of the spinners' activity on the aggregation dynamics by applying different rotational frequencies, Re = 0.1, 0.72 and 3.58, to spinners embedded in passive matrixes of ϕ_A = 0.8. In agreement with our previous observations for the spinner–spinner interaction in passive environments,[36,37] we observe there exists a minimum threshold of loading stress, or spinner activity, for the spinner attractive interaction to be important. Spinners rotating at Re smaller than 0.1 do not aggregate. At these activities, the stress applied to the passive monolayer is not large enough to promote the occurrence of yielding events, which ultimately result in spinner aggregation.[36] On the contrary, spinners rotating at Re $\geq$ 0.72 do aggregate, and the higher the rotational frequency, the faster the evolution of the system. Interestingly, the dynamic scaling exponent of the spinner aggregation seems to be independent of the rotational frequency, as shown in Fig. 6. However, the range of the initial dynamical regime, which probably corresponds to the fastest growing unstable composition mode, shifts towards shorter times. The spinner–spinner attraction in passive matrixes follows activated dynamics.[37] The monolayer region in between the two spinners (*i.e.* the bridge) needs to be loaded before it yields, which has an associated time scale. This time scale depends on the mechanical properties and configuration of the monolayer. If the stress applied by the spinners overcomes this time scale, the passive particle mobility increases, resulting in yielding events, which leads to the erosion or degradation of the bridge.[36] Therefore, the higher the rotational frequency of the spinners (*i.e.* Re), the shorter time required to stress the bridge and thus as the frequency of the spinners increases the faster the growth of the clusters at short time scales. The differences observed between the experiment and simulations on Re come from the approximations made in our simulation model. For example, in our simulations the momentum transfer between the spinner and neighboring particles comes exclusively from the fluid, while in the experiment friction and collision between particles may play an important role in transferring momentum.

We further investigate the microscopic details of the spinner aggregation process by tracking the active clusters over time, noting when clusters collide, initial separation distances between clusters which merge, and the velocity at which clusters approach, as shown in Fig. 7. In Fig. 7A, the velocity at which spinner clusters approach as a function of cluster size is presented. We observe that there is a maximum velocity associated with a cluster size of approximately 45 μm. This behavior of the cluster velocity as a function of size reveals two competing effects involved in the mobility of the clusters, and therefore their aggregation. The effect which opposes spinner aggregation is the effective drag, which opposes the movement of the clusters through the monolayer, and the drag increases with cluster size. Meanwhile the stress that the spinner cluster can exert on the monolayer increases with the size of the cluster. This increases the frequency of the yielding events resulting in the degradation of the bridge and spinner aggregation. In addition, we observe that the range of the attractive interaction between clusters,

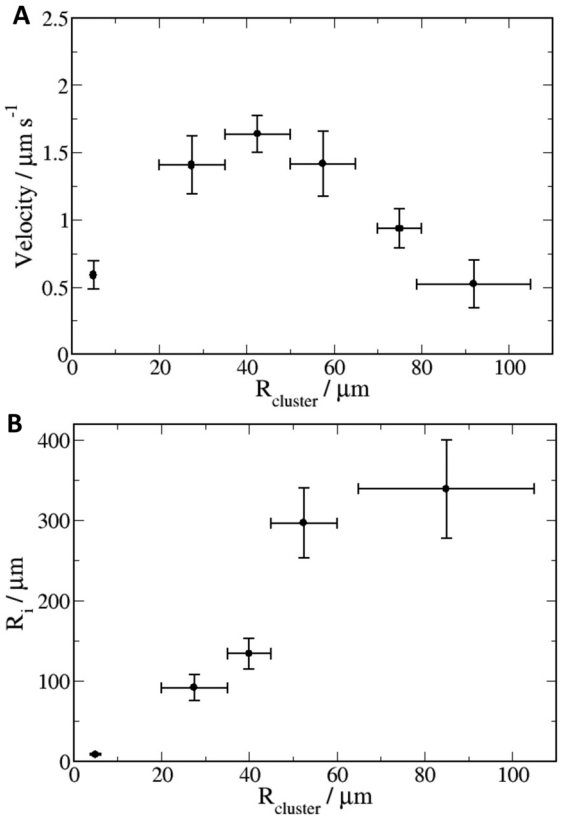

Fig. 7 (A) Average approach velocity of the active clusters as a function of the cluster size (*i.e.* radius of the cluster). (B) Range of the attractive interaction between active clusters as a function of the cluster size. Error bars correspond to the standard deviation of the trials.

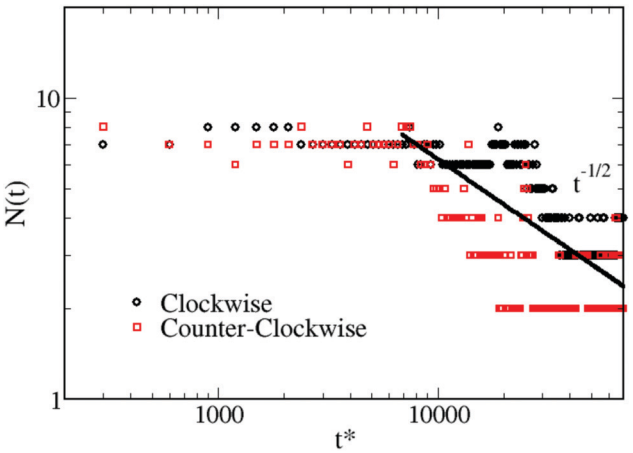

Fig. 8 Aggregation dynamics of spinners rotating clockwise (black circles) at a concentration of 2.47%, and counter-clockwise (red squares) at a concentration of 2.47% within a passive monolayer of ϕ_A = 0.8. t^* corresponds to the dimensionless time $t{\cdot}\omega$.

R_i, increases with the cluster size, as shown in Fig. 7B. Individual spinner clusters were tracked and as the clusters collide and form bigger clusters the initial distance between colliding clusters was calculated and plotted as a function of the average radius of the two colliding clusters. As discussed above, the stress exerted on the monolayer increases with the cluster size. Therefore, this increase in the applied stress on the monolayer results in higher mobility of the passive particles of the monolayer, which results in longer range interactions.

Finally, we explore the behavior of a ternary mixture in which a passive monolayer is doped with a symmetric mixture of spinners rotating in opposite senses, clockwise and counter-clockwise. In our previous work, we demonstrated that while two co-rotating spinners embedded in a passive matrix experience an attractive interaction, counter-rotating spinners exhibit a repulsive interaction in dense passive environments.[36] We observe that spinners in dense passive monolayers tend to form clusters of co-rotating particles and thus we observe the formation of three different phases: (i) passive particles, (ii) spinners rotating clockwise and (iii) spinners rotating counter-clockwise, as shown in Fig. 8. This is the result of the attractive interaction between spinners rotating in the same direction and the repulsive interaction between spinners rotating in opposite directions. Interestingly, again we see a scaling factor of $t^{1/2}$ for this system as well which is reminiscent of source limited coarsening. A similar system composed of a ternary mixture of co-rotating, counter-rotating, and passive particles has been previously investigated;[27,29] however the aggregation dynamics were not reported for this system so there is no comparison to be made.

4 Conclusions

We studied the aggregation of active rotating particles embedded in a passive monolayer. We demonstrate that the non-equilibrium attractive interaction between spinners within dense passive matrixes[36,37] results in their aggregation. This aggregation resembles 2D coarsening,[53] which has also been described for other pure active systems.[48,49] The experimental system seems to exhibit coarsening behavior reminiscent of the diffusion limited scenario, while the simulation appears similar to the source limited case. This difference may be due to the lack of magnetic interactions in the simulations. Although the system size we can reach does not allow us to unambiguously determine the dynamic scaling exponent of the spinner aggregation process, we explore the effect of the particle area fraction of the monolayer, spinner concentration and spinner activity on the aggregation behavior. We observe that the monolayer must behave as a solid, $\phi_A > 0.7$, in order to observe spinner aggregation. In addition, for the spinners to stress the monolayer and thus produce yielding events that result in the attraction of spinners, there is a minimum activity threshold, Re > 0.1, in simulations. Interestingly, the aggregation dynamics seems to be independent of the spinner concentration. We also study the microscopic details of the cluster aggregation. We observe that spinner clusters move faster as the size increases up to a velocity maximum at around $R_{cluster}$ = 45 μm. Finally, we show that a ternary mixture of passive particles and co-rotating and counter-rotating spinners results in the formation of clusters of spinners with the same sense of rotation. This is the result of the attractive interaction between spinners rotating in the same

direction, and the repulsive interaction between spinners rotating in opposite directions. Interestingly, again we see a scaling factor of $t^{1/2}$ for this system as well which is reminiscent of source limited coarsening.

Conflicts of interest

There are no conflicts to declare.

Acknowledgements

This work was supported by Department of Energy BES award #ER46919 (theoretical and simulation work) and the Chang Family (experimental work).

References

1 J. D. Gunton, M. San Miguel and P. Sahni, *Phase Transition and Critical Phenomena*, Academic, London, 1983, vol. 8.
2 J. W. Cahn, *Acta Metall.*, 1961, **9**, 795–801.
3 J. W. Cahn and J. E. Hilliard, *J. Chem. Phys.*, 1958, **28**, 258–267.
4 J. Palacci, S. Sacanna, A. P. Steinberg, D. J. Pine and P. M. Chaikin, *Science*, 2013, **339**, 936–940.
5 L. Corté, P. M. Chaikin, J. P. Gollub and D. J. Pine, *Nat. Phys.*, 2008, **4**, 420–424.
6 T. Ishikawa and T. J. Pedley, *Phys. Rev. Lett.*, 2008, **100**, 088103.
7 A. P. Berke, L. Turner, H. C. Berg and E. Lauga, *Phys. Rev. Lett.*, 2008, **101**, 038102.
8 K. Drescher, K. C. Leptos, I. Tuval, T. Ishikawa, T. J. Pedley and R. E. Goldstein, *Phys. Rev. Lett.*, 2009, **102**, 168101.
9 J. Buhl, D. J. T. Sumpter, I. D. Couzin, J. J. Hale, E. Despland, E. R. Miller and S. J. Simpson, *Science*, 2006, **312**, 1402–1406.
10 N. C. Darnton, L. Turner, S. Rojevsky and H. C. Berg, *Biophys. J.*, 2010, **98**, 2082–2090.
11 A. Ordemann, G. Balazsi and F. Moss, *Phys. A*, 2003, **325**, 260–266.
12 Y. Wu, A. D. Kaiser, Y. Jiang and M. S. Alber, *Proc. Natl. Acad. Sci. U. S. A.*, 2009, **106**, 1222–1227.
13 H. P. Zhang, A. Be'er, E.-L. Florin and H. L. Swinney, *Proc. Natl. Acad. Sci. U. S. A.*, 2010, **107**, 13626–13630.
14 S.-N. Lin, W.-C. Lo and C.-J. Lo, *Soft Matter*, 2014, **10**, 760–766.
15 J. Toner and Y. Tu, *Phys. Rev. E: Stat. Phys., Plasmas, Fluids, Relat. Interdiscip. Top.*, 1998, **58**, 4828–4858.
16 M. Ballerini, N. Cabibbo, R. Candelier, A. Cavagna, E. Cisbani, I. Giardina, V. Lecomte, A. Orlandi, G. Parisi, A. Procaccini, M. Viale and V. Zdravkovic, *Proc. Natl. Acad. Sci. U. S. A.*, 2008, **105**, 1232–1237.
17 A. Cavagna, A. Cimarelli, I. Giardina, G. Parisi, R. Santagati, F. Stefanini and M. Viale, *Proc. Natl. Acad. Sci. U. S. A.*, 2010, **107**, 11865–11870.
18 J. L. Silverberg, M. Bierbaum, J. P. Sethna and I. Cohen, *Phys. Rev. Lett.*, 2013, **110**, 228701.
19 B. Szabó, G. J. Szöllösi, B. Gönci, Z. Jurányi, D. Selmeczi and T. Vicsek, *Phys. Rev. E: Stat., Nonlinear, Soft Matter Phys.*, 2006, **74**, 061908.
20 D. F. Hinz, A. Panchenko, T.-Y. Kim and E. Fried, *Soft Matter*, 2014, **10**, 9082–9089.
21 H. Wioland, F. G. Woodhouse, J. Dunkel, J. O. Kessler and R. E. Goldstein, *Phys. Rev. Lett.*, 2013, **110**, 268102.
22 T. Sanchez, D. T. N. Chen, S. J. DeCamp, M. Heymann and Z. Dogic, *Nature*, 2012, **491**, 431–434.
23 J.-F. Joanny and S. Ramaswamy, *Nature*, 2010, **467**, 33–34.
24 J. E. Martin and A. Snezhko, *Rep. Prog. Phys.*, 2013, **76**, 126601.
25 J. Yan, S. C. Bae and S. Granick, *Soft Matter*, 2015, **11**, 147–153.
26 N. Kumar, H. Soni, S. Ramaswamy and A. K. Sood, *Nat. Commun.*, 2014, **5**, 4688.
27 K. Yeo, E. Lushi and P. M. Vlahovska, *Soft Matter*, 2016, **12**, 5645–5652.
28 K. Yeo, E. Lushi and P. M. Vlahovska, *Phys. Rev. Lett.*, 2015, **114**, 188301.
29 N. H. P. Nguyen, D. Klotsa, M. Engel and S. C. Glotzer, *Phys. Rev. Lett.*, 2014, **112**, 075701.
30 M. Spellings, M. Engel, D. Klotsa, S. Sabrina, A. M. Drews, N. H. P. Nguyen, K. J. M. Bishop and S. C. Glotzer, *Proc. Natl. Acad. Sci. U. S. A.*, 2015, **112**, E4642–E4650.
31 B. C. V. Zuiden, J. Paulose, W. T. M. Irvine, D. Bartolo and V. Vitelli, *Proc. Natl. Acad. Sci. U. S. A.*, 2016, **113**, 12919–12924.
32 G. Kokot, S. Das, R. G. Winkler, G. Gompper, I. S. Aranson and A. Snezhko, *Proc. Natl. Acad. Sci. U. S. A.*, 2017, **114**, 12870–12875.
33 M. Han, J. Yan, S. Granick and E. Luijten, *Proc. Natl. Acad. Sci. U. S. A.*, 2017, **114**, 7513–7518.
34 C. Scholz, M. Engel and T. Pöschel, *Nat. Commun.*, 2018, **9**, 931.
35 A. P. Petroff, X.-L. Wu and A. Libchaber, *Phys. Rev. Lett.*, 2015, **114**, 158102.
36 J. L. Aragones, J. P. Steimel and A. Alexander-Katz, *Nat. Commun.*, 2016, **7**, 11325.
37 J. P. Steimel, J. L. Aragones, H. Hu, N. Qureshi and A. Alexander-Katz, *Proc. Natl. Acad. Sci. U. S. A.*, 2016, **113**, 4652–4657.
38 J. Jover, A. J. Haslam, A. Galindo, G. Jackson and E. A. Muller, *J. Chem. Phys.*, 2012, **137**, 144505.
39 B. Dünweg and A. Ladd, *Adv. Polym. Sci.*, 2008, 1–78.
40 E.-J. Ding and C. K. Aidun, *J. Stat. Phys.*, 2003, **112**, 685.
41 A. J. C. Ladd, *J. Fluid Mech.*, 1994, **271**, 285.
42 M. Kalontarov, M. T. Tolley, H. Lipson and D. Erickson, *Microfluid. Nanofluid.*, 2010, **9**, 551–558.
43 J. H. E. Promislow, A. P. Gast and M. Fermigier, *J. Chem. Phys.*, 1995, **102**, 5492.
44 J. Richardi and J.-J. Weis, *J. Chem. Phys.*, 2011, **135**, 124502.
45 Y. Gao, M. A. Hulsen, T. G. Kang and J. M. J. den Toonder, *Phys. Rev. E: Stat., Nonlinear, Soft Matter Phys.*, 2012, **86**, 041503.
46 C. Reynolds, D. Robinson, D. Aarts, M. Wilson, W. Sampson and R. Dullens, *Europhys. Lett.*, 2016, **116**, 28001.

47 C. P. Reynolds, MSc thesis, University of Oxford, 2016.
48 S. Dey, D. Das and R. Rajesh, *Phys. Rev. Lett.*, 2012, **108**, 238001.
49 G. S. Redner, M. F. Hagan and A. Baskaran, *Phys. Rev. Lett.*, 2013, **110**, 055701.
50 E. Climent, K. Yeo, M. R. Maxey and G. E. Karniadakis, *J. Fluids Eng.*, 2007, **129**, 379–387.
51 B. A. Grzybowski, X. Jiang, H. Stone and G. M. Whitesides, *Phys. Rev. E: Stat., Nonlinear, Soft Matter Phys.*, 2001, **64**, 011603.
52 B. Grzybowski, H. Stone and G. Whitesides, *Nature*, 2000, **405**, 1033–1036.
53 K. Binder and D. Stauffer, *Phys. Rev. Lett.*, 1974, **33**, 1006–1009.
54 B. Meerson, *Rev. Mod. Phys.*, 1996, **68**, 215–257.
55 T. Mason and D. Weitz, *Phys. Rev. Lett.*, 1995, **74**, 1250–1253.
56 T. G. Mason, *Rheol. Acta*, 2000, **39**, 371–378.
57 Y. Goto and H. Tanaka, *Nat. Commun.*, 2016, **6**, 1–10.